Remote Dipolar Interactions for Objective Density Calibration
and Flow Control of Excitonic Fluids

Kobi Cohen,[1] Ronen Rapaport,[1,*] and Paulo V. Santos[2]

[1]*Racah Institute of Physics, The Hebrew University of Jerusalem, Jerusalem 91904, Israel*
[2]*Paul-Drude-Institut für Festkörperelektronik, Hausvogteiplatz 5-7, 10117 Berlin, Germany*
(Received 27 October 2010; published 23 March 2011)

In this Letter we suggest a method to observe *remote* interactions of spatially separated dipolar quantum fluids, and in particular, of dipolar excitons in GaAs bilayer based devices. The method utilizes the static electric dipole moment of trapped dipolar fluids to induce a local potential change on spatially separated test dipoles. We show that such an interaction can be used for model-independent, objective fluid density measurements, an outstanding problem in this field of research, as well as for interfluid exciton flow control and trapping. For a demonstration of the effects on realistic devices, we use a full two-dimensional hydrodynamical model.

Dipolar quantum fluids are very intriguing physical entities that are intensively sought for in various material systems, such as ultracold polar molecules [1] and excitons in semiconductor bilayer structures [2,3]. The interest in such fluids arises from the basic unresolved questions regarding their possible rich thermodynamic phases, which are predicted to emerge from the interplay between their quantum statistics and the particular form of the dipole-dipole interaction [4–6]. While the local interactions between nearby dipoles is expected to determine the physical state of the fluid, it should be interesting to observe the effect of interactions between spatially remote fluids. This concept of remote interactions can also be utilized, as we will suggest here, to determine in an objective, model-independent way the density of a dipolar fluid, a tricky "boot-strap" problem especially for excitons in bilayer systems. It can also be utilized as a method to control the flow of one fluid by other, remotely located fluids.

As mentioned above, dipolar fluids can be realized for excitons in bilayer structures. An exciton consists of a Coulomb bound electron-hole pair inside a semiconductor, forming a bosonlike quasiparticle. In electrically gated GaAs coupled quantum wells (CQWs), also known as bilayer structures, an externally applied electric field, using semitransparent electrical gates, results in the creation of two-dimensional dipolar excitons. These light mass excitonic quasiparticles have their electron and hole constituents separated into two layers [Fig. 1(a)] and thus have an increased lifetime, an elevated quantum-degeneracy temperature (compared to atoms or molecules), and all carry a dipole moment oriented perpendicular to the quantum well (QW) plane. The two-dimensional dipolar excitons (X_d) interact with each other via the repulsive dipole-dipole forces, and therefore exciton-based systems can be used to explore a low dimensional interacting fluid hydrodynamics at quantum-degeneracy conditions. The X_d can also be transformed back into light signals in a controlled way

by switching the external gate's electric field, and thus can potentially be used for unique functional optoelectronic devices. Various methods can also be used to effectively transport and manipulate X_d flows. Indeed, in the past few years several groups introduced relatively efficient ways of controlling X_d fluxes, by using electric field gradients [7], surface acoustic waves [8] and modulated gate voltages [9–11]. Transport of excitons has also been measured in other bilayer systems [12–14]. However, all of the above methods are based on external manipulations and not on the internal state of the device. This may limit future functionality of devices based on exciton fluids.

Another crucial experimental difficulty, which is important in the aspect of the fundamental understanding of the X_d fluid thermodynamics, is to independently and accurately estimate the density of X_d created inside a sample. Such an estimate is vital for correctly identifying and gaining physical insight into phenomena such as phase transitions, quantum degeneracy, and particle correlations. This task however, turns out to not be straightforward. The current method for estimating X_d densities is to deduce
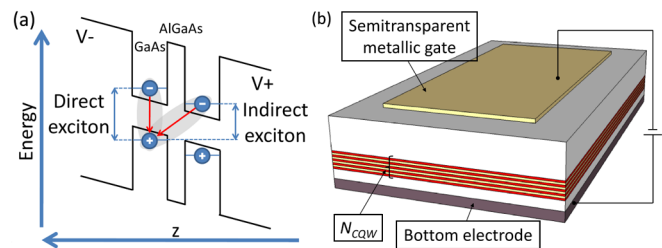
FIG. 1 (color online). (a) A Schematic band diagram for a GaAs/AlGaAs CQW structure, showing the formation of direct and indirect (dipolar) excitons. (b) A sketch of the proposed sample structure, containing a stack of CQWs (their number is marked by N_{CQW}), a homogeneous back electrode and a semitransparent top electric gate. The specific gate geometries for the various implementations discussed in the text are given in Fig. 2.

it from measurements of the energy shift ("blueshift") of recombining X_d photoluminescence (PL). This energy shift strongly depends on the local density correlations around the recombining excitons, which in turn depends on the thermodynamic state of the fluid [6,15]. Therefore this method relies on a knowledge of the fluid state, which makes this density calibration method a strongly model-dependant, boot-strap process. Finally, we note that while dipole-dipole interactions have been observed to affect the properties and the dynamics of a dipolar fluid locally, the remote effect of a collection of such dipoles on a system spatially separated from it has not been observed as far as we know. This concept alone is worthwhile pursuing.

Here, we propose that remote interactions between spatially separated excitons can be observed in both spectroscopy and hydrodynamics experiments. Such an observation can also be used for resolving practical current challenges: in the first part of the Letter we describe a scheme that utilizes remote interactions for an objective, model-independent dipolar fluid density measurements which does not depend on local density correlations, and in the second part we describe a method to manipulate dipolar fluids using their remote interactions. We note that while we present the implementation of the concept for dipolar exciton fluids in electrostatic traps, the concept developed here is quite general and can be implemented in other types of trapping devices and also for different types of dipolar fluids.

As a starting point for our discussion, one has to consider a trap region which will confine the X_d in the QW plane, and oppose their spreading due to diffusion and repulsive interaction. Various ways for trapping dipolar excitons have been realized in the past few years [16–18]. The approach we took in the current work utilizes electrostatic traps, which have a flat potential profile and a sharp boundary [19,20], leading to a flat average density distribution of excitons in the trap *on a macroscopic scale*, denoted here by n (note that local, microscopic density inhomogeneities are always expected due to dipole-dipole interactions [6]). These electrostatic gates can also define narrow channels, in which excitons can propagate only in one direction [21]. In the following discussion, we consider a sample containing a vertical stack of separated CQWs [Fig. 1(b)]. The number of CQWs is denoted by N_{CQW}. As will be shown hereafter, increasing N_{CQW} will increase the effect of the remote interactions. We let d denote the dipole length, i.e., the spatial separation of the electron and hole wave functions in each CQW along the z axis, $\vec{r}$ is a radius vector in the QW plane denoting the position of a test dipole, and $\vec{r}_x$ is an arbitrary point inside the trapping region. In terms of the interaction energy $U_d(\vec{r} - \vec{r}_x)$ between two dipoles separated by a distance $|\vec{r} - \vec{r}_x|$, the total interaction energy for a test dipole at a point $\vec{r}$ is given by [6]:

$$E_d(\vec{r}) = N_{CQW} \times n \iint_{trap} U_d(\vec{r} - \vec{r}_x) g_d(\vec{r} - \vec{r}_x) d^2 r_x, \quad (1)$$

where $g_d(\vec{r} - \vec{r}_x)$ is the pair correlation function and $n g_d(\vec{r} - \vec{r}_x) d^2 r_x$ is the average number of X_d's within an area $d^2 r_x$ at a distance $|\vec{r} - \vec{r}_x|$ from the test dipole. It is clear that $E_d(\vec{r})$ for any $\vec{r}$ inside the trap strongly depends on the shape of the correlation function g_d. Therefore, extracting n from a local measurement of $E_d(\vec{r})$ requires an independent knowledge of g_d. This is the essence of the objective density calibration problem. However, $g_d(\vec{r} - \vec{r}_x)|_{|\vec{r} - \vec{r}_x| \to \infty} = 1$, as at large distances all local correlations disappear. Hence, for a test dipole remotely located from the rest of the trapped X_d fluid, as shown schematically in Fig. 2(a), Eq. (1) reduces to:

$$E_d(\vec{r}) = N_{CQW} \times n \iint_{trap} U_d(\vec{r} - \vec{r}_x) d^2 r_x. \quad (2)$$

Under such conditions, the dependence of $E_d(\vec{r})$ on g_d vanishes and no knowledge of the form of g_d is required to extract n from a measurement of $E_d(\vec{r})$.

To check this concept of dipolar fluid density measurements in realistic devices, we consider the geometry shown in Fig. 2(b). By applying two different voltages on the circular probe gate and the electrostatic ring trap surrounding it, two potential wells for the dipolar excitons in the QW plane are formed, one under each gate. Because of the radial gap between the two separated electrodes, these potential wells are spatially separated by a narrow barrier. Furthermore, as these potential wells have different depths (due to different applied gate voltages V_1 and V_2), their corresponding X_d PL can be spectrally separated [19].
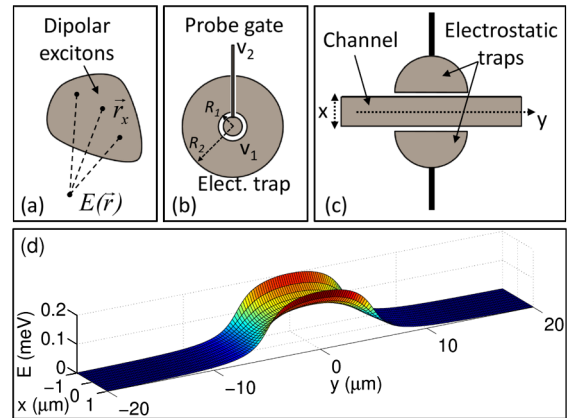
FIG. 2 (color online).   (a) The remote interaction energy E at a point $\vec{r}$ is calculated by integrating the contribution from X_d contained inside a specified region. (b) A proposed exciton density measurement device. The detected emission energy of X_d trapped inside the inner probe gate is shifted due to the interaction with X_d in the outer trap. V_1 and V_2 are the applied voltages on the probe and outer trap, respectively. (c) A sketch of a flow device containing a narrow channel, surrounded by two half-circular electrostatic traps. (d) A numerical calculation of the energy profile along a 2 μm-wide channel of the device in (c), formed by X_d in the two surrounding 10 μm diameter electrostatic traps, which are located 1 μm away from the channel edges. Here, $d = 16$ nm, $N_{CQW} = 4$ and $n = 10^{11}$ cm^{-2}.

A straightforward calculation for E_d in this case using Eq. (2) yields the result:

$$E_d(\vec{r} = 0) = N_{CQW} 2\pi \frac{ne^2d^2}{\epsilon} \left(\frac{1}{R_1} - \frac{1}{R_2} \right), \quad (3)$$

where R_1 and R_2 are the inner and outer radii of the electrostatic ring trap, respectively, and we have used $U_d = e^2d^2/(\epsilon|\vec{r} - \vec{r}_x|^3)$, where ϵ is the QW dielectric constant. This approximation for U_d is valid if $|\vec{r} - \vec{r}_x| \gg d$ for every $\vec{r}_x$, which is the case we are considering here. Increasing N_{CQW} linearly increases the effective density at each point $\vec{r}_x$ and thus the interaction strength [22]. For $N_{CQW} = 5$, $n = 10^{11}$ cm^{-2}, $d = 20$ nm, $R_1 = 4$ μm, $R_2 = 50$ μm, Eq. (3) gives $E_d \approx 0.3$ meV. This E_d term can be detected in the PL line blueshift of the probe X_d, and can be used to deduce the X_d density n inside the outer trap, as all other parameters are known. Since the microscopic density correlation scale r_c is typically smaller or of the order of the interparticle distance $\sim n^{-1/2}$, we have that $R_1, R_2 \gg r_c$. As a result, this is a model-independent density measurement, as it does not assume anything on the local state of the X_d fluid in the outer ring. The only assumption is that n is constant on the macroscopic scale of the trap area, which was already experimentally verified [19,20].

While in the first part we showed that the effect of remote dipolar interactions can be observed spectroscopically, we now suggest a hydrodynamic effect through the concept of flow control using remote interactions. We consider a flow device schematically shown in Fig. 2(c). Here, a 2 μm-wide channel gate is surrounded by two half-circular electrostatic traps with a 10 μm diameter each, located 1 μm away from the channel edges. The traps are loaded with a steady state density n. Applying Eq. (2) to all points inside the channel yields an interaction energy profile, shown in Fig. 2(d). For typical experimental parameters $d = 16$ nm, $n = 10^{11}$ cm^{-2}, $N_{CQW} = 4$ and $\epsilon = \epsilon_{GaAs} = 13$, the energy "bump" peak has a value of $E_b \approx 0.15$ meV.

We now use an extension of the device shown in Fig. 2(c) to demonstrate efficient trapping of X_d in a channel. This extension is described in Fig. 3, where the trapping scheme consists of a narrow channel, but with four adjacent half-circular electrostatic control traps. The control traps are loaded with a steady state X_d density (by, e.g., continuous wave excitation) which can be tuned to control the energy profile along the channel, denoted by $E(\vec{r})$. The traps' location thus defines a trapping region along the channel (marked by A).

To study the dynamics of the proposed device, we use a numerical integration of the exciton hydrodynamics equation [23,24]:

$$\frac{\partial n}{\partial t} + \nabla(\vec{J}_D + \vec{J}_d + \vec{J}_{ext}) + \frac{n}{\tau} = 0. \quad (4)$$

Here, n and τ denote the spatially dependent X_d density and lifetime, respectively. The terms appearing inside the brackets are the diffusion induced current $\vec{J}_D = -D\nabla n$,

the dipolar repulsion induced current $\vec{J}_d = -n\mu\alpha\nabla n$, and a current due to external forces $\vec{J}_{ext} = n\mu\nabla E$, where μ is the exciton mobility and α is a material and structure parameter [24]. We also assumed a uniform temperature of the excitons throughout the sample. The principle of remote interactions is demonstrated by trapping freely expanding X_d inside the one-dimensional channel, as described in Fig. 3. The double-bump energy profile along the channel is created by loading the control traps with X_d [Fig. 3(a)]. An initial Gaussian distribution spot $n_i(\vec{r}) = n_i \exp(-4r^2)$ of X_d is created inside the channel at $t = 0$ [Fig. 3(b)], and the system evolves in time according to Eq. (4) for $t_f = 2$ μs. The resulting X_d density profiles [Figs. 3(c) and 3(d)] show that the X_d are much better confined along the channel when the control traps are loaded (trapping "on").

To characterize and quantify the performance of such a flow control device, we analyzed the same device configuration described in Fig. 3, but under various conditions. Figures 4(a)–4(c) show the resulting X_d's density profile, $n_f(\vec{r})$, along the channel, normalized to the maximal initial X_d density n_i, and its dependence on E_b, n_i and the temperature T. One can see that n_f increases with the bump height E_b, and decreases with the initial X_d's density n_i and temperature T [25]. An objective measure for
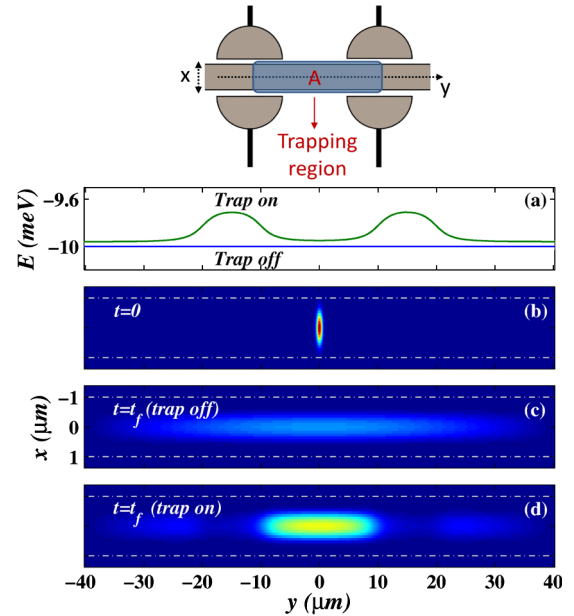
FIG. 3 (color online). Upper panel: a proposed trapping scheme that consists of a narrow channel along the y direction, and 4 adjacent control traps. The effective trapping region, A, is marked by the shaded rectangle. Lower panels: (a) The energy profile along the channel with trapping on (green line), and off (blue line). (b) Initial X_d distribution in the channel at $t = 0$. The dashed lines mark the channel edges. The resulting X_d distribution for $t_f = 2$ μs is shown (color scale ×50) for (c) trapping "off" (empty control traps) and (d) trapping "on" (occupied control traps), showing a strong suppression of the X_d spreading along the channel.
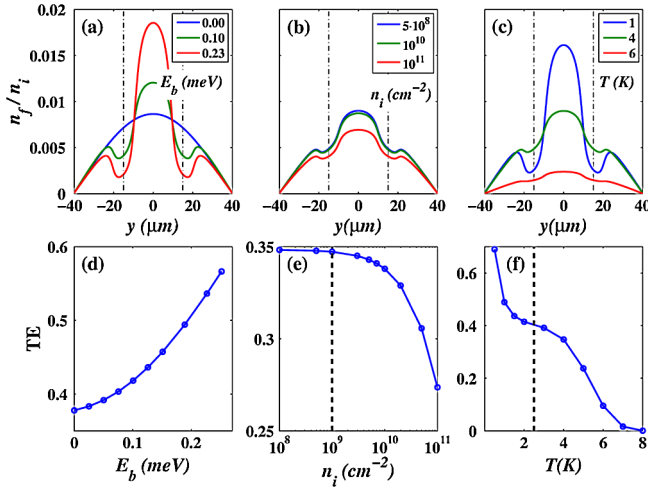
FIG. 4 (color online).   The normalized X_d density, n_f/n_i, at $t_f = 2$ μs for changing (a) bump height E_b, (b) initial density n_i and (c) temperature T. The trapping efficiency TE as a function of the same parameters as in (a)–(c) is shown in (d)–(f). The dashed lines in (e) and (f) mark the density and temperature, respectively, where $\vec{J}_{ext} \approx \vec{J}_d + \vec{J}_D$.

quantifying the performance of the device is the effective trapping efficiency (TE), defined as

$$\text{TE} = \frac{\int_A n_f(\vec{r})d^2\vec{r}}{\int_A n_i(\vec{r})d^2\vec{r}} \exp(t_f/\tau), \qquad (5)$$

where the integral is over the trapping area A (as marked in Fig. 3) and the factor $\exp(t_f/\tau)$ compensates for the recombination loss of particles due to their finite lifetime τ, thus making the above definition of TE a time-independent one (excluding other loss mechanisms such as boundary effects). The results show that there is an increase in TE when E_b is raised [Fig. 4(d)], and a decrease in TE with increasing n_i [Fig. 4(e)] and increasing temperature [Fig. 4(f)].

We can qualitatively understand these results by means of comparing the different X_d currents. For an energy bump E_b with a typical width W, the induced current is estimated by $\vec{J}_{ext} = n\mu\nabla E \approx n_i\mu E_b/W$, while for an initial X_d density profile $n_i(\vec{r})$ with typical width L, the dipolar repulsion current will be $\vec{J}_d = -n\mu\alpha\nabla n \approx \mu\alpha n_i^2/L$. The characteristic diffusion current, using the Einstein relation for a low density, nondegenerate Bose gas [23], is given by $\vec{J}_D = -D\nabla n \approx \mu k_B T n_i/L$. One expects that the trapping efficiency should fall whenever the size of the external trapping current $\vec{J}_{ext}$ becomes smaller than internal expanding currents $\vec{J}_{int} = \vec{J}_d + \vec{J}_D$, i.e., when $|\vec{J}_{ext}/\vec{J}_{int}| \lesssim 1$. As is shown here, the behavior of the analyzed system follows this rule of thumb fairly well. For the given experimental conditions (with $L/W \approx 3$), the dashed line in Fig. 4(e) marks the initial density where $\vec{J}_{ext} \approx \vec{J}_d + \vec{J}_D$, and the dashed line in Fig. 4(f) marks the temperature where $\vec{J}_{ext} \approx \vec{J}_d + \vec{J}_D$. There is a substantial decrease in TE upon increasing density [Fig. 4(e)] and increasing temperature [Fig. 4(f)] above these lines.

These simple and intuitive results can be implemented in the design of devices for trapping and flow control of excitons. For example, one can build a flow device by applying a voltage gradient along a channel [7], and switch the flow on and off by remote dipole interactions with X_d fluids in the control traps, in a device similar to the one depicted in Fig. 2(c).

In summary, we propose a method for new dipolar exciton flow devices, which utilizes the remote interactions between spatially separated dipolar exciton fluids. It allows for a direct and model-independent density calibration measurement, as well as for excitonic fluid-fluid control and manipulation. Such a concept is quite general and can possibly be implemented in different types of dipolar fluids and other device schemes.

*ronenr@phys.huji.ac.il
[1] L. Santos et al., Phys. Rev. Lett. **85**, 1791 (2000).
[2] D. Snoke, Science **298**, 1368 (2002).
[3] J. P. Eisenstein and A. H. MacDonald, Nature (London) **432**, 691 (2004).
[4] H. P. Büchler et al., Phys. Rev. Lett. **98**, 060404 (2007).
[5] G. E. Astrakharchik et al., Phys. Rev. Lett. **98**, 060405 (2007).
[6] B. Laikhtman and R. Rapaport, Phys. Rev. B **80**, 195313 (2009).
[7] A. Gärtner et al., Appl. Phys. Lett. **89**, 052108 (2006).
[8] J. Rudolph, R. Hey, and P. V. Santos, Phys. Rev. Lett. **99**, 047602 (2007).
[9] A. A. High et al., Science **321**, 229 (2008).
[10] G. Grosso et al., Nat. Photon. **3**, 577 (2009).
[11] Y. Y. Kuznetsova et al., Opt. Lett. **35**, 1587 (2010).
[12] I. B. Spielman et al., Phys. Rev. Lett. **84**, 5808 (2000).
[13] E. Tutuc, M. Shayegan, and D. A. Huse, Phys. Rev. Lett. **93**, 036802 (2004).
[14] Z. Vörös et al., Phys. Rev. Lett. **97**, 016803 (2006).
[15] C. Schindler and R. Zimmermann, Phys. Rev. B **78**, 045313 (2008).
[16] S. Zimmermann et al., Phys. Rev. B **56**, 13 414 (1997).
[17] A. T. Hammack et al., Phys. Rev. Lett. **96**, 227402 (2006).
[18] A. T. Hammack et al., J. Appl. Phys. **99**, 066104 (2006).
[19] R. Rapaport et al., Phys. Rev. B **72**, 075428 (2005).
[20] G. Chen et al., Phys. Rev. B **74**, 045309 (2006).
[21] A. Gärtner et al., Phys. Rev. B **76**, 085304 (2007).
[22] The linear dependence of Eq. (2) on N_{CQW} is correct as long as the vertical size of the CQW stack is much smaller than the minimal in-plane distance $|\vec{r} - \vec{r}_x|$, a condition which can easily be met.
[23] A. L. Ivanov, Europhys. Lett. **59**, 586 (2002).
[24] R. Rapaport and G. Chen, J. Phys. Condens. Matter **19**, 295207 (2007).
[25] For varying E_b, we used $n_i = 10^9$ cm^{-2} and $T = 1.5$ K. In the case of varying the initial densities, we used $E_b = 0.125$ meV and $T = 4$ K. For varying temperatures, we set $n_i = 10^9$ cm^{-2} and $E_b = 0.125$ meV.